

## Two liquid states of matter: A dynamic line on a phase diagram

V. V. Brazhkin,<sup>1,\*</sup> Yu. D. Fomin,<sup>1</sup> A. G. Lyapin,<sup>1</sup> V. N. Ryzhov,<sup>1</sup> and K. Trachenko<sup>2</sup>

<sup>1</sup>*Institute for High Pressure Physics RAS, 142190 Troitsk Moscow Region, Russia*

<sup>2</sup>*South East Physics Network and School of Physics, Queen Mary University of London, Mile End Road, London E1 4NS, United Kingdom*

(Received 15 August 2011; published 30 March 2012)

It is generally agreed that the supercritical region of a liquid consists of one single state (supercritical fluid). On the other hand, we show here that liquids in this region exist in two qualitatively different states: “rigid” and “nonrigid” liquids. Rigid to nonrigid transition corresponds to the condition  $\tau \approx \tau_0$ , where  $\tau$  is the liquid relaxation time and  $\tau_0$  is the minimal period of transverse quasiharmonic waves. This condition defines a new dynamic crossover line on the phase diagram and corresponds to the loss of shear stiffness of a liquid at all available frequencies and, consequently, to the qualitative change in many important liquid properties. We analyze this line theoretically as well as in real and model fluids and show that the transition corresponds to the disappearance of high-frequency sound, to the disappearance of roton minima, qualitative changes in the temperature dependencies of sound velocity, diffusion, viscous flow, and thermal conductivity, an increase in particle thermal speed to half the speed of sound, and a reduction in the constant volume specific heat to  $2k_B$  per particle. In contrast to the Widom line that exists near the critical point only, the new dynamic line is universal: It separates two liquid states at arbitrarily high pressure and temperature and exists in systems where liquid-gas transition and the critical point are absent altogether. We propose to call the new dynamic line on the phase diagram “Frenkel line”.

DOI: [10.1103/PhysRevE.85.031203](https://doi.org/10.1103/PhysRevE.85.031203)

PACS number(s): 65.20.De, 62.10.+s, 63.50.-x, 66.20.Cy

### I. INTRODUCTION

Our current understanding and discussion of basic states of matter such as solid, liquid, and gas is illustrated by “temperature, pressure” ( $T, P$ ) or “temperature, density” ( $T, \rho$ ) phase diagrams. Crossing a line on such diagrams corresponds to thermodynamic phase transitions, leading to qualitative changes in the physical behavior of the system. Below, we show that, for one basic state of matter, the liquid phase, an equally important qualitative change in system behavior exists, which is related to the change in its dynamics rather than thermodynamics. Consequently, we propose that all liquids have two qualitatively different states, and that a new additional crossover line (narrow zone) should be added to the phase diagram which separates the two states. This line does not correspond to any thermodynamic phase transition, i.e., it is a crossover, and there is no discontinuity of any physical properties along the line. We called it the “Frenkel line” as discussed below.

More specifically, a typical ( $T, P$ ) diagram [Fig. 1(a)] implies that a liquid is separated from a gas by the boiling line ending at the critical point. The diagram further implies that only one single state (frequently called “supercritical fluid”) exists for all pressures and temperatures above the critical point. On the other hand, we propose that an important qualitative change in a fluid behavior takes place on crossing our new line. Importantly, this dynamical crossover line extends for arbitrary values of pressure and temperature above the critical point [Fig. 1(a)]. In addition, the new line is not related to the critical point from the physical perspective and, therefore, exists in systems where the liquid-gas transition is absent altogether as is the case in some soft-matter subjects with short-range attractive forces as well as in the model soft-sphere system [Fig. 1(b)].

We begin our discussion with the paper of Frenkel [1], who provided a microscopic description of Maxwell phenomenological viscoelastic theory of liquid flow [2] by introducing liquid relaxation time  $\tau$ :  $\tau$  is the average time between two consecutive atomic jumps in a liquid at one point in space. Each jump can approximately be viewed as a jump of an atom from its neighboring cage into a new equilibrium position with subsequent cage relaxation. These atomic jumps give a liquid its ability to flow. The relaxation time  $\tau$  is a fundamental flow property of a liquid, and it defines liquid viscosity  $\eta$  and diffusion coefficient  $D$ .

The above picture implies that the motion of an atom in a liquid consists of two types: quasiharmonic vibrational motion around an equilibrium position as in a solid and diffusive motion between two neighboring positions where typical diffusion distances exceed vibrational distances by about a factor of 5–10 [ Figs. 2(a)–2(c)]. Therefore, atomic motion in a liquid combines both elements of the short-amplitude vibrational motion as in a solid and the large-amplitude ballistic-collisional motion as in a gas. One should mention that Frenkel’s ideas were discussed and used for the past 20 years by Wallace [3] and Chisolm and Wallace [4] to calculate the thermodynamic and dynamic properties of a liquid.

In this paper, we propose that the point at which the *solid-like oscillatory motion ceases*, leaving only the gaslike motion, marks the change in the most important properties of a fluid.

### II. THE FRENKEL LINE ON THE PHASE DIAGRAM

The value of  $\tau$  decreases with temperature increase, spanning many orders of magnitude. On the other hand, the minimal (Debye) vibration period,  $\tau_0$  ( $\tau_0 \approx 0.1$ – $1$  ps), is weakly temperature dependent and is mostly defined by interactions in a given system. At certain high temperatures, the solidlike vibration character ceases [Figs. 2(a), 2(d), and 2(e)]. This

\*brazhkin@hppi.troitsk.ru

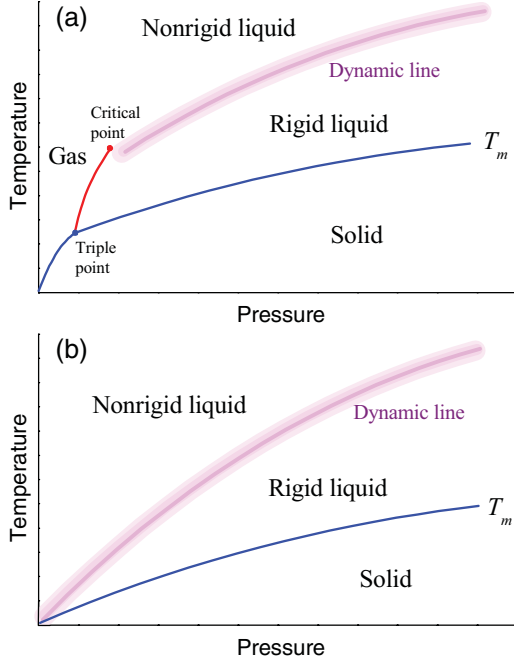


FIG. 1. (Color online) Pressure-temperature phase diagrams (in arbitrary units) of (a) an ordinary substance and (b) a system without the boiling line and liquid-gas critical point. In both cases, there exists a dynamic line separating rigid and nonrigid liquids.

point is reached when  $\tau$  becomes comparable to  $\tau_0$ ,

$$\tau \approx \tau_0. \quad (1)$$

The sign of the approximate equality means that the values can differ by tens of percent. In the following discussion, we consider  $\tau$  as the average time it takes an atom to move the average interparticle distance  $a$ . Then,  $\tau$  quantifies the motion envisaged by Frenkel where an atom jumps distance  $a$  during time  $\tau$  between two equilibrium positions at low temperatures as well as the motion at high temperatures where two equilibrium positions are absent altogether and the motion between collisions is ballistic as in a gas.

We note that, for  $\tau > \tau_0$  where dynamics is mostly vibrational, the atomic jumps take place by activation over the barrier created by the potential energy of interaction [1]. Therefore, the transition from solidlike vibrations to continuous gaslike ballistic motion takes place when kinetic energy  $K$  of a particle becomes comparable to the potential energy of their interaction. Hence, condition (1) implies that approximately,

$$3k_B T/2 \approx E_{\text{pot}}. \quad (2)$$

For most substances, the ratio of kinetic to potential energy  $K/E_{\text{pot}}$  at the melting temperature is significantly lower than 1. In this case, the particles are primarily within the range of the quasiharmonic potential and, after melting, relatively long-lived regions with a well-defined vibration spectrum and short-range order remain. We will elaborate on this below.

Condition (1) is achieved on a certain new crossover line on the phase diagram. Below, we show that crossing this line leads to important qualitative changes in the system behavior

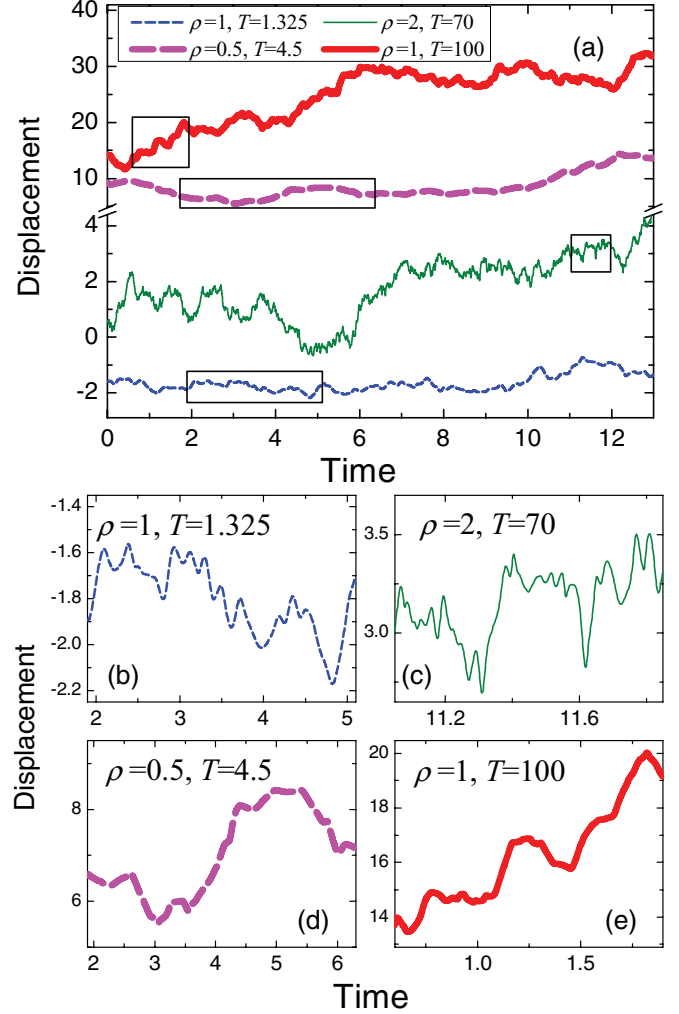


FIG. 2. (Color online) Examples of particle trajectories ( $x$  coordinate) for the LJ liquid at different conditions, presented in LJ units ( $\rho_c = 0.314$ ,  $T_c = 1.31$ ). Panels (b)–(e) show selected fragments from (a). Cases (b) and (c) correspond to the rigid state where vibrations are present (thin lines); (d) and (e) correspond to collisional motion in the nonrigid state (thick lines). Time and displacement are in standard LJ units.

as witnessed by the change in its elastic, structural, dynamic, diffusive, and thermodynamic properties.

### III. SOLIDLIKE ELASTIC AND STRUCTURAL PROPERTIES OF A LIQUID

An important insight from the introduction of relaxation time is that, if observation time is smaller than  $\tau$ , the local structure of a liquid does not change and is the same as that of a solid. This enabled Frenkel to predict that a liquid should maintain solidlike shear waves at all frequencies  $\omega > 2\pi/\tau$  [1]. This prediction was later confirmed experimentally for different kinds of liquids [5–8].

The maximum oscillation frequency available in the system is  $\omega_0 = 2\pi/\tau_0$ . Therefore, solidlike shear waves exist in the range of  $2\pi/\tau < \omega < 2\pi/\tau_0$ . Consequently, condition (1) ( $\tau \approx \tau_0$ ) corresponds to the complete loss of shear waves and,

therefore, to the loss of shear resistance, or rigidity, at all frequencies existing in the system.

We note that the condition of the crossover (1) and other conditions considered below correspond to approximate equality. Moreover, there are wide distributions of the  $\tau$  and  $\tau_0$  values, and we consider their average values. Nevertheless, in all liquids, there are definite  $T, P$  conditions corresponding to the loss of transverselike vibrations in the excitation spectra, hence, we can speak about the definite line or, at least, about the narrow crossover instead of a wide crossover.

Usually, the sharp transition in the macroscopic system is associated with some divergent value. The condition (1) defines the crossover in the dynamics of a system. To propose a more or less strict criterion of the transition, one can consider the analogy with percolation. Let us consider the high-temperature state of a fluid. If, for time  $\tau$ , the projection of the particle momentum on its total displacement changes sign at least once, then this particle is considered an oscillating one. A small fraction of these particles will be present even in the low-density gas state. The proportion of such particles increases with the temperature decrease, and at a certain temperature, the infinite percolation cluster consisting of these particles appears. We can assume that this temperature corresponds to the appearance of the first high-frequency transverse-like excitations in the fluid. Of course, depending on the shape of the distributions of the  $\tau$  and  $\tau_0$  values, this percolation occurs at  $\tau \approx \tau_0$  where the proportionality coefficient can differ from 1 by a dozen percent.

The ability of liquids to flow is often associated with zero rigidity, or shear resistance, that markedly distinguishes liquids from solids. However, this implies zero rigidity at low frequencies only, whereas, at higher frequencies, a liquid supports shear stress. On the other hand, condition (1) marks the qualitative change, from the physical point of view, in system elastic properties: shear resistance is lost completely at all frequencies available in the liquid. Therefore, condition (1) marks the crossover between a “rigid” liquid where rigidity exists in a certain frequency range and a “nonrigid” liquid which cannot sustain rigidity at any frequency.

The crossover (1) has important implications for the ability of liquids to undergo phase transitions, an emerging and fast-developing area of research [9–11]. When  $\tau > \tau_0$  at low temperatures, local structure or definite short-range order structure (SROS) of the liquid remains unchanged during times shorter than  $\tau$ . In this case, pressure and temperature changes can induce a phase transition in a liquid, accompanied by the change in the SROS and dynamics. On the other hand, when  $\tau < \tau_0$  at high temperatures, only the random packing structure type can exist because atoms are in the continuous gaslike state of motion. In this case, pressure can only induce a change in density but not a phase transition with a change in SROS. Therefore, the Frenkel line demarcates the regions on the phase diagram where phase transitions in a liquid operate.

#### IV. DYNAMICS AND SOUND PROPAGATION

The qualitative change in atomic dynamics, defined by Eq. (1), has important consequences for sound propagation and diffusion. Let us approach the liquid from low temperatures where  $\tau > \tau_0$ . The speed of sound in a liquid or a solid  $V_s$

is defined from the dispersion relation  $\omega = V_s k$ . Using linear Debye approximation and taking maximum frequency  $\omega$  as Debye frequency  $\omega_0 = 2\pi/\tau_0$  and  $k_{\max} = \pi/a$  gives  $V_s = 2a/\tau_0$ . Let us now approach the fluid from high temperatures where the oscillatory motion is lost and recall that  $\tau$  is the time between two consecutive collisions over distance  $a$ . Then,  $V_{\text{th}} \approx a/\tau$ , where  $V_{\text{th}}$  is the particle thermal velocity. Therefore, condition (1) implies

$$V_s \approx 2V_{\text{th}}. \quad (3)$$

In condensed phases, such as solids and liquids, the speed of sound is primarily determined by the interactions between atoms: The sound velocities are given by elastic moduli. In dense liquids, moduli vary insignificantly with temperature along isochors [12], and sound velocities are weakly temperature dependent. On the other hand, the thermal velocity of a classical particle increases with temperature without bound. Therefore, a temperature range must exist where the speed of sound and thermal velocity become comparable in magnitude. The physical meaning of condition (3) is that particles cease to feel elastic resistance of the medium and start moving in a ballistic way.

The condition for thermal velocity of the particles becoming half the speed of sound as a condition for the change in atomic dynamics is quite natural. The factor of 2 arises from the fact that the neighboring particles move in opposite phases at the highest frequency, and their relative thermal velocity equals the speed of sound.

The speed of sound in the nonrigid liquid is defined by thermal velocity, such as in a gas, and this speed should increase with the temperature on isobars. On the other hand, the speed of sound in the rigid liquid decreases with temperature due to the decrease in the bulk modulus on isobars. Thus, on isobars near the line defined by the conditions (1) and (3), the qualitative change in the temperature dependence of the sound velocity should take place.

We note that Eq. (3) is based on the same physical grounds as Eq. (2). Indeed, the speed of sound is governed by the elastic moduli, which are, in turn, proportional to the potential energy of the system per unit volume. However, the proportionality coefficient in Eq. (2) may be significantly (several times) different from 1. Indeed, the elastic moduli are the second derivatives of the potential energy, i.e., the nature of the interparticle interaction is very important for the proportionality coefficient. For example, in Ref. [13], it was shown that a van der Waals fluid near the critical point holds  $k_B T \approx E_{\text{pot}}$ , while a Coulomb plasma with a compensating background near the critical point holds  $3k_B T \approx E_{\text{pot}}$ .

Another interesting consequence of Eq. (1) is related to the phenomenon of “high-frequency sound” or positive dispersion of sound velocity, which is the increase in the speed of sound at high frequencies. Frenkel predicted [1] that this effect should exist for frequencies  $\omega > 2\pi/\tau$ . If, as he argued, shear waves kick in at frequency  $2\pi/\tau$ , the speed of sound increases from  $(B/\rho)^{1/2}$  to  $[(B + 4G/3)/\rho]^{1/2}$ , where  $B$  is the bulk modulus and  $G$  is the shear modulus of a liquid because  $G$  becomes nonzero at this frequency. For viscous liquids, such behavior has been indeed observed many times in the past 50 years (see, for example, Ref. [8]). The viscoelastic model was later developed in detail, including

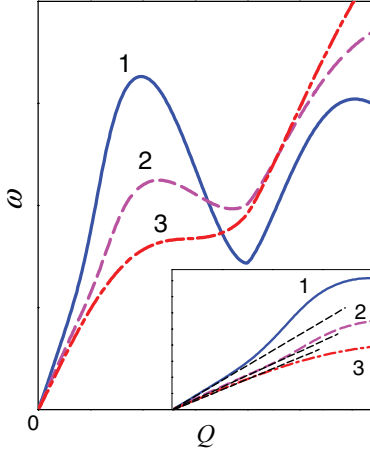


FIG. 3. (Color online) Schematic dispersion curves for longitudinal excitations in a liquid at different temperatures and fixed pressure. Curves 1–3 correspond to temperatures below, in the vicinity, and above the dynamical line, respectively ( $T_1 < T_2 < T_3$ ). The inset shows the initial parts of the same curves where the black straight dashed lines indicate initial slopes of the dispersion curves.

memory function formalism, nonlocal mode coupling theory, etc. [14–18]. Following the prediction, the high-frequency sound was recently observed in numerous simple nonviscous liquids, receiving particular attention since the development of inelastic x-ray techniques [19–22]. We now observe that the proposed crossover (1) marks the point at which the positive dispersion disappears completely because, as discussed above, this crossover corresponds to the complete loss of shear waves that can exist in a liquid and corresponding loss of the high-frequency sound (see Fig. 3).

Another important feature of the liquid excitation spectra is the presence of a rotonlike minimum of the dispersion curve in a second pseudo-Brillouin zone [19] (see Fig. 3). At the crossover, defined by the condition (1), the contributions of jumping “ballistic” atoms and “vibrating” atoms become comparable to each other, and the rotonlike minimum disappears (see Fig. 3 for the illustration of the general trend).

## V. DIFFUSION, VISCOSITY, AND THERMAL CONDUCTIVITY

The change in the character of atomic diffusion in the liquid at the crossover (1) occurs at a particular value of diffusion constant  $D^*$ .  $D$  can be estimated as  $D = a^2/6\tau$ . When  $\tau \approx \tau_0$  at the crossover (1), we have

$$D \approx D^* \approx a^2/6\tau_0. \quad (4)$$

Taking  $a \approx 1 \text{ \AA}$  and  $\tau_0 \approx 0.1 \text{ ps}$  gives  $D^* \approx 10^{-8} \text{ m}^2/\text{s}$ . The condition  $D = D^*$  provides a good estimation of the dynamic line defined by condition (1) because it is fairly insensitive to the increases in pressure and temperature. Indeed, both  $a^2$  and  $\tau_0$  decrease with pressure only slightly, and their ratio becomes even less sensitive to pressure and temperature. We note that the  $D^*$  value is consistent with the experimental values of diffusion near critical point  $D_c$  [12]. Indeed, not far from the critical point, liquids are known to lose their elastic properties, and the relaxation process changes its nature from an activation

to a collisional one [23,24], hence, the near equality of  $D^*$  and  $D_c$  is not surprising in our picture. Thus, for a rather crude estimation of the crossover (1) at moderate pressures, we can use the condition,

$$D \approx D_c. \quad (5)$$

In this sense, the proposed dynamic line starts not far from the end of the liquid-gas transition. However, it is important to stress that all basic conditions above, Eqs. (1)–(4), are not related to the liquid-gas transition and to the existence of a critical point from the physical point of view and continue to operate in systems where the critical point is absent altogether. We will further comment on this below.

Importantly, condition (1) corresponds to the crossover between two different qualitative temperature dependencies of diffusion  $D$  and viscosity  $\eta$ . Indeed, when  $\tau > \tau_0$  at low temperatures,  $\tau \sim \exp(U/T)$ , where  $U$  is the effective activation barrier. Then,  $D \sim a^2/\tau \sim \exp(-U/T)$ . On the other hand, when  $\tau < \tau_0$  at high temperatures,  $\tau$  quantifies thermal motion as discussed above:  $\tau \sim 1/V_{\text{th}} \sim 1/T^{1/2}$ , giving  $D \sim T^{1/2}$  for a low-density gas or  $D \sim T^\alpha$ , where  $\alpha$  is almost constant for a dense fluid [25]. Therefore, condition (1) gives the crossover of  $D$  from exponential to power-law temperature dependence.

Similar to  $D$ , temperature behavior of viscosity  $\eta$  changes at the crossover (1). Indeed, when  $\tau > \tau_0$ ,  $\eta$  decreases with temperature almost exponentially, which can be seen most easily by applying the Maxwell relation  $\eta = G_\infty \tau$ , where  $G_\infty$  is the instantaneous shear modulus having weak temperature dependence in comparison with the exponential decrease in  $\tau$ . On the other hand, when  $\tau < \tau_0$ ,  $\eta \sim T^{1/2}$ . This follows from applying either the Stokes-Einstein-Debye relationship  $\eta \sim T/D$  or the Maxwell relationship  $\eta = G_\infty \tau$ , where  $\tau \sim 1/T^{1/2}$  from above and recalling that  $G_\infty$  is proportional to the kinetic  $\sim T$  term in this regime [26]. We, therefore, conclude that condition (1) corresponds to the qualitative change in the temperature behavior of viscosity as it crosses over from the exponential decrease at  $\tau > \tau_0$  to the power-law increase at  $\tau < \tau_0$ .

Thermal conductivity  $\kappa$  is another important physical property that should have a minimum close to the crossover (1). Indeed, usually, thermal conductivity behaves similar to viscosity. The value  $\kappa$  can be estimated as  $\kappa \sim c_V V L$ , where  $c_V$  is the constant-volume specific heat,  $V \approx V_s$  for the rigid liquid,  $V \approx V_{\text{th}}$  for the nonrigid liquid, and  $L$  is the free path length of the phonon or atom, correspondingly. When  $\tau > \tau_0$ ,  $\kappa$  decreases with temperature because  $L$  and  $c_V$  decrease. On the other hand, when  $\tau < \tau_0$ ,  $\kappa \sim V_{\text{th}} \sim T^{1/2}$  since  $L$  and  $c_V$  values have a weak temperature dependence in the nonrigid liquid.

We, therefore, conclude that three important physical values—viscosity, thermal conductivity, and sound velocity should have minima on the isobars in the vicinity of the crossover line.

## VI. THERMAL ENERGY AND SPECIFIC HEAT

Experimentally, constant-volume specific heat of liquids at ambient pressure decreases from about  $3k_B$  per particle around the melting temperature to about  $2k_B$  at high temperatures [12,27]. A further decrease in specific heat with a temperature

increase up to gaslike values  $3k_B/2$  is observed at high pressures in the supercritical region [12]. This behavior was quantitatively explained on the basis of decreasing the contribution of transverselike modes to liquid energy with the temperature [28]. In this model, the liquid thermal energy per atom is

$$\frac{E}{N} = k_B T \left[ 3 - \left( \frac{\tau_0}{\tau} \right)^3 \right]. \quad (6)$$

According to Eq. (6), when  $\tau$  considerably exceeds  $\tau_0$  at low temperatures, liquid energy is close to  $3k_B T$  per atom, giving the Dulong-Petit value of specific heat of  $3k_B$ . When  $\tau$  approaches  $\tau_0$  at high temperatures, liquid energy becomes  $2k_B T$  per atom, giving the specific heat of  $2k_B$ , consistent with the experimental results. At this temperature, shear waves are completely lost at all frequencies, and longitudinal modes only contribute to the heat capacity. Therefore, the crossover from a rigid to a nonrigid liquid at  $\tau \approx \tau_0$  is accompanied by the decrease in the specific heat from its solid-state value to the value of  $2k_B$ ,

$$c_V \approx 2k_B. \quad (7)$$

Equation (7) gives the minimal value of specific heat that a rigid liquid can possibly have. A further decrease in heat capacity corresponds to the loss of longitudinal modes as the temperature is increased until the dense gas state (nonrigid liquid) is reached with  $c_V = 3k_B/2$ .

Having discussed the main physical properties that change at the crossover (1), we now provide numerical and experimental evidence supporting our proposal.

## VII. EVIDENCE FROM MOLECULAR DYNAMICS SIMULATIONS AND EXPERIMENTAL DATA

We have drawn the lines determined by conditions (1), (2), (3), (5), and (7), for real substances (Ar, Ne, and  $N_2$ ) and model particle systems with Lennard-Jones (LJ) and soft-sphere potentials (SSps) (Figs. 4 and 5). Details of molecular dynamics (MD) simulations are given in the Appendix.

It is well known that the LJ potential adequately represents the behavior of many molecular and rare gas liquids, whereas, SSs systems describe a behavior of many real substances at very high pressures where an attractive term of the interparticle potential can be neglected. We have calculated points on the phase diagram that correspond to strict equalities  $\tau = \tau_0$ ,  $3kT/2 = E_{\text{pot}}$ ,  $V_s = 2V_{\text{th}}$ ,  $D = D_c$ , and  $c_V = 2k_B$ , hence, moderate differences between the lines are not unexpected as discussed above.

According to Fig. 4, the position of the crossover line [condition (1)] for the Lennard-Jones system agrees with the line determined by condition (5) at moderate pressures  $P < 10 - 10^2 P_c$  and with the lines determined by conditions (3) and (7) at high pressures  $P > 10 P_c$ . At low pressures, the lines determined by conditions (3) and (7) shift from the crossover line (1) due to critical point anomalies and loss of Debye approximation at low densities. As discussed above, condition (2) is not directly based on condition (1), and the proportionality coefficient in Eq. (2) differs from 1 significantly [for LJ particles,  $3kT/2 \approx 5E_{\text{pot}}$ , for SSs particles

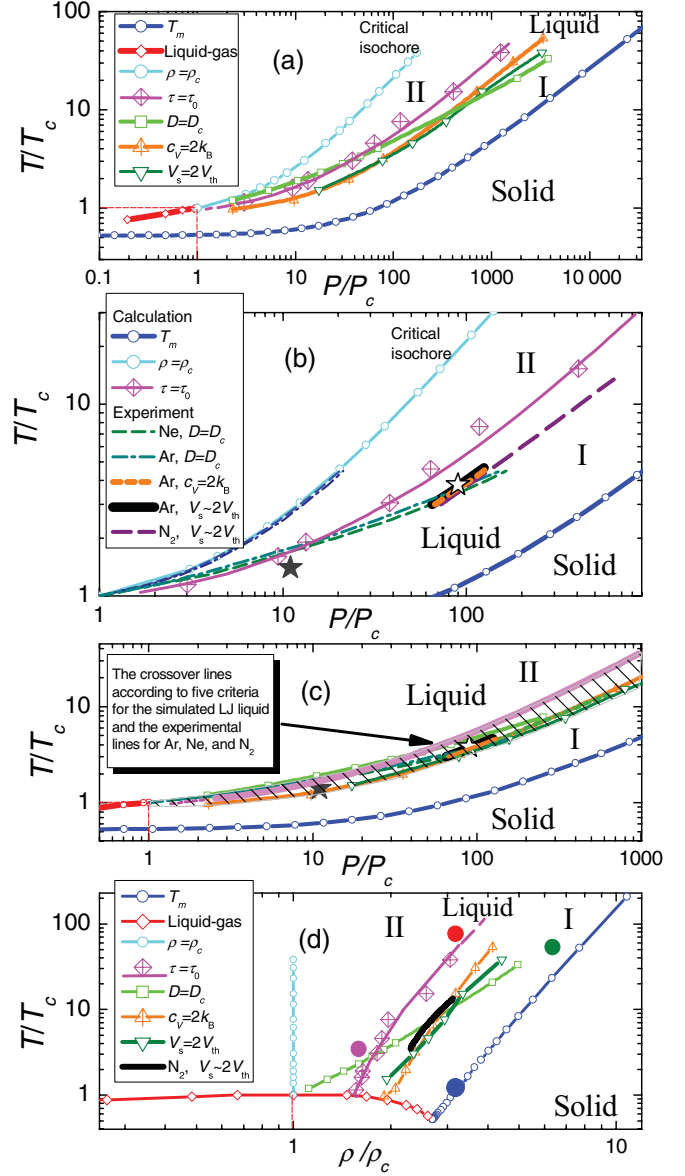


FIG. 4. (Color online) (a)–(c)  $(T, P)$  phase diagram and (d)  $(T, \rho)$  phase diagram of the LJ liquid in the relative critical coordinates. Panels (a) and (d) present calculated lines defined by different criteria (see the text). Panel (b) presents some experimental data from Ref. [12]. Stars in panel (b) correspond to known experimental points where the liquid loses shear waves and positive dispersion (open symbol for Ar [20] and solid symbol for  $N_2$  [22]). Experimental critical isochors are also shown in panel (b) (dashed olive line for Ne and dashed-dotted olive line for Ar). Experimental data for criterion (3) for nitrogen and points (solid circles) from the simulation of the LJ system in Fig. 2 (with the same color) are shown in panel (d). Panel (c) illustrates a narrow crossover zone according to different criteria for the LJ system and real liquids. In all cases, number I corresponds to the rigid liquid, and number II corresponds to the nonrigid one. In panel (d), the density from the liquid side is shown for the melting curve.

( $n = 6$ ),  $3kT/2 \approx 0.3E_{\text{pot}}$ ]. For a soft-sphere system, the lines determined by conditions (1), (3), and (7) match well over the entire pressure range (Fig. 5) as no critical point and associated anomalies exist for this system.

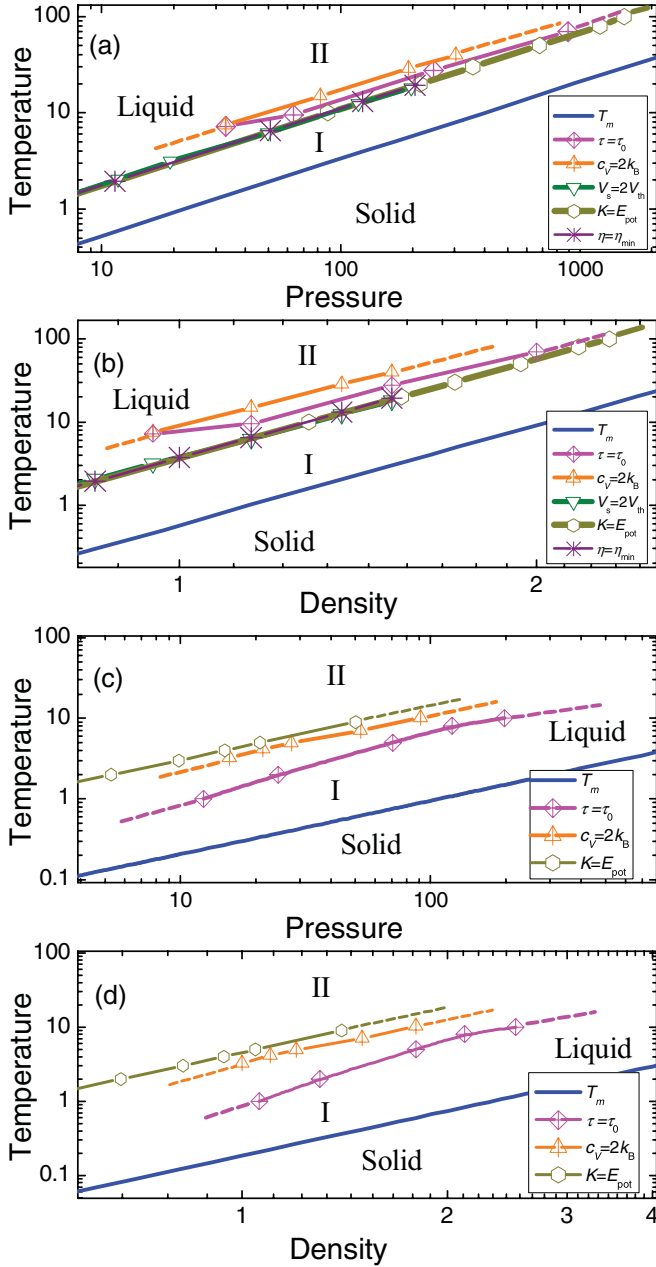


FIG. 5. (Color online)  $(T,P)$  and  $(T,\rho)$  phase diagrams of the simulated soft-sphere systems with (a) and (b)  $n = 12$  and (c) and (d)  $n = 6$ . This figure presents calculated lines defined by different criteria including those for the minimum of viscosity  $\eta$  along the isochor in panel (b). In panels (b) and (d), the density from the liquid side is shown for the melting curve. Pressure, density, and temperature are in standard soft-sphere units.

In addition to model systems, we find good agreement between the theoretical predictions and experimental data for liquid Ar, Ne, and  $N_2$  (Fig. 4). In particular, we observe a good match between the region of the disappearance of the positive dispersion of sound velocity in liquid Ar [20] and  $N_2$  [22] and the dynamic line (Fig. 4).

Despite the approximate way in which conditions (2), (3), (5), and (7) correspond to condition (1), all the lines defined by different conditions are located within quite a narrow range. We note that these lines are located at temperatures

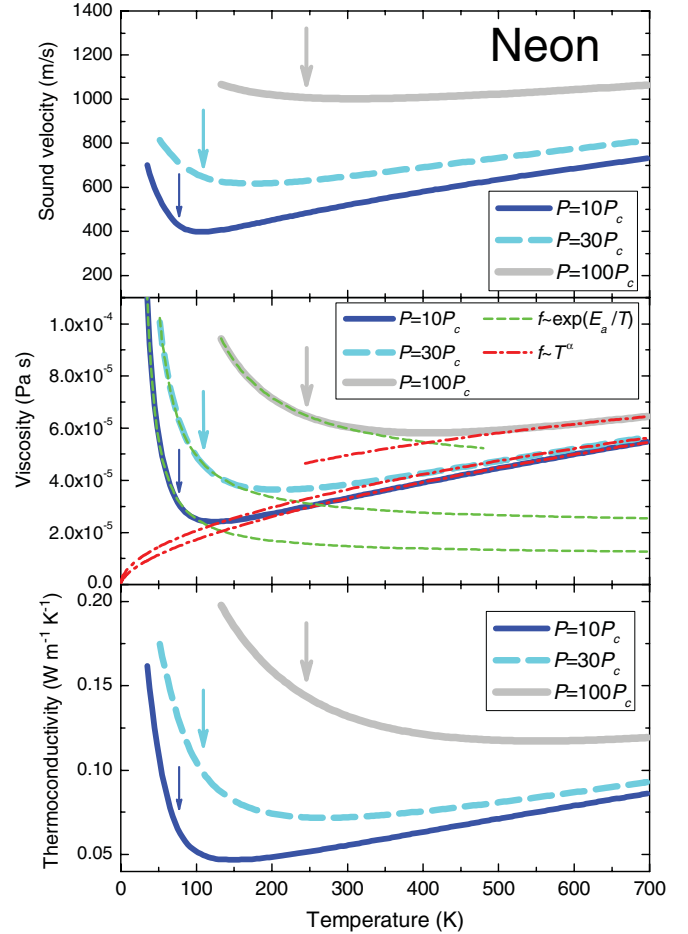


FIG. 6. (Color online) Experimental [12] isobaric temperature dependences of sound velocity, viscosity, and thermal conductivity of neon. Asymptotes for viscosity at low and high temperatures correspond to exponents of inverse temperature and power law, respectively. Arrows indicated the corresponding temperatures of condition (1),  $\tau = \tau_0$ . The exponent  $\alpha = 0.59$  at  $P = 10P_c$ ,  $0.52$  at  $P = 30P_c$ , and  $0.32$  at  $P = 100P_c$ .

that are significantly above the melting line, implying that the new line separates two distinct liquid states. We also note that this Frenkel line is located significantly below the isochore, in contrast to the Widom line discussed below in more detail. Importantly, the lines of all conditions [with the exception of condition (5), which is approximate and is valid only at moderate pressures] lie almost parallel to each other in the whole range of pressures and temperatures. Notably, pressure in this range varies by almost 4 orders of magnitude. We further observe that, by only a slight variation in the proportionality coefficients in criteria (1), (3), and (5), namely, by a factor of 1.3–1.4, the lines defined by these conditions practically coincide, which testifies to the commonality of physical mechanisms underlying the above criteria. The line of criterion (7) coincides with the main line [criterion (1)] for  $c_V = 1.9k_B$ , which differs from  $c_V = 2k_B$  by 5% only.

The qualitative change in the temperature dependence of sound velocity  $V_{sl}$ , viscosity  $\eta$ , and thermal conductivity  $\kappa$  for real substances (Ne,  $N_2$ ) also occurs near the crossover line (Figs. 6 and 7). In fact, condition (1) holds close to the

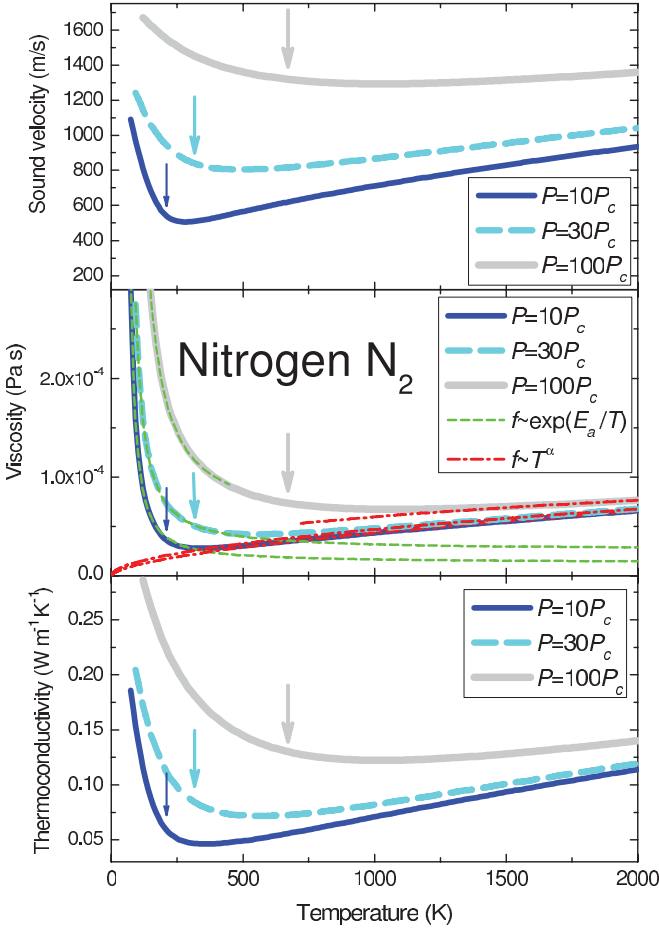


FIG. 7. (Color online) Experimental [12] isobaric temperature dependences of sound velocity, viscosity, and thermal conductivity of nitrogen. Asymptotes for viscosity at low and high temperatures correspond to exponents of inverse temperature and power law, respectively. Arrows indicated the corresponding temperatures of condition (1),  $\tau = \tau_0$ . The exponent  $\alpha = 0.59$  at  $P = 10P_c$ ,  $0.53$  at  $P = 30P_c$ , and  $0.31$  at  $P = 100P_c$ .

temperature where the deviation from the exponential viscosity decrease starts. It means that activated behavior operates even if a particle exhibits one oscillation before jumping to another position.

The temperature dependencies of the constant-volume heat capacity for Ar (along isobars) and for the LJ liquid (along isochors) are presented in Fig. 8. The dynamic crossover in both cases is located at condition (7) when  $c_V = 1.9k_B$ .

One can mention that, in most of real metallic, covalent, and ionic liquids, the Frenkel line lies at extreme experimental conditions, e.g.,  $\sim 10$  GPa and  $\sim 10^4$  K, and only shock-wave experiments can be used for its study. However, for molecular and rare-gas liquids, the line is situated at the “static pressure” experimental conditions. For example, condition (1) for Ne at  $P \sim 3$  GPa should take place at  $T \sim 1100$  K (approximately five to six times higher than the melting temperature). For many soft-matter systems, such as colloidal systems, macromolecules, etc., the dynamic line lies in the accessible range of pressures and temperatures as well.

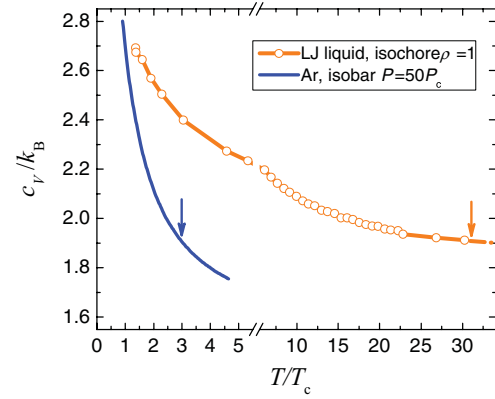


FIG. 8. (Color online) The dependencies of heat capacity versus temperature for the LJ liquid along the isochore (for  $\rho = 1$ ) (orange circles with interpolation lines) and for Ar along isobar  $P = 50P_c$  (blue solid line). The arrows indicate the points of intersection of the corresponding curves by the Frenkel line according to the condition (1).

### VIII. THE FRENKEL LINE AND THE MELTING LINE

Interestingly, all crossover lines correspond to a density increase with increasing temperature: The relation  $\rho \sim T^k$  is met, where  $k \approx 0.25$  for liquid  $N_2$ , Lennard-Jones, and soft-sphere systems with  $n = 12$  (Figs. 4 and 5). We recall that, for any system of particles with a uniform potential, there are scaling relations for physical values [29]. In particular,  $\rho^{n/3}/T = \text{const}$  along the melting line for the soft-sphere system, giving  $\rho \sim T_m^{1/4}$  for the melting temperature  $T_m$  for  $n = 12$  [29]. The similarity in the dependence of  $\rho(T)$  for the melting and dynamic lines implies similar scaling relations for the dynamic line. This point will be discussed in detail elsewhere. As a result, the region of the rigid liquid does not, under any pressures, disappear (Figs. 4 and 5). Consequently, the Frenkel line continues for arbitrarily high pressures and temperatures.

It should be mentioned that the “softer” the repulsion potential, the wider the region of existence of a rigid liquid (Fig. 5). We have calculated the ratio between the kinetic energy of the particles and the potential energy of the particle interaction  $K/E_{\text{pot}}$  along the melting curve for the soft-sphere system with different repulsion coefficients  $n$  (see Fig. 9). This ratio is almost constant along the melting curve and varies from 0 for  $n = 3$  to infinity for  $n \rightarrow \infty$  (hard spheres). The value of  $K/E_{\text{pot}}$  near the melting curve is considerably larger than 1 for only very large coefficients  $n > 30$ . For even larger values of  $n$ , the dynamic line can hide behind the melting curve. Particularly, the condition (7),  $c_V = 2k_B$ , is fulfilled near the melting curve with  $n \approx 60$  (see Fig. 10). Thus, for  $n > 50$ – $60$ , the dynamic line falls within the region of crystal stability and separates a low-temperature almost harmonic state of the crystal and a high-temperature strongly anharmonic state. In the high-temperature state, a particle moves, most of the time, in a ballistic way outside the region of the action of the potential, similar to the behavior of the particles of a hard-sphere crystal for which the potential energy is equal to zero and  $c_V = 3k_B/2$ . In this case, the condition (1),  $\tau \approx \tau_0$ , practically implies that a particle in the crystal spends similar time moving (almost) harmonically and ballistically.

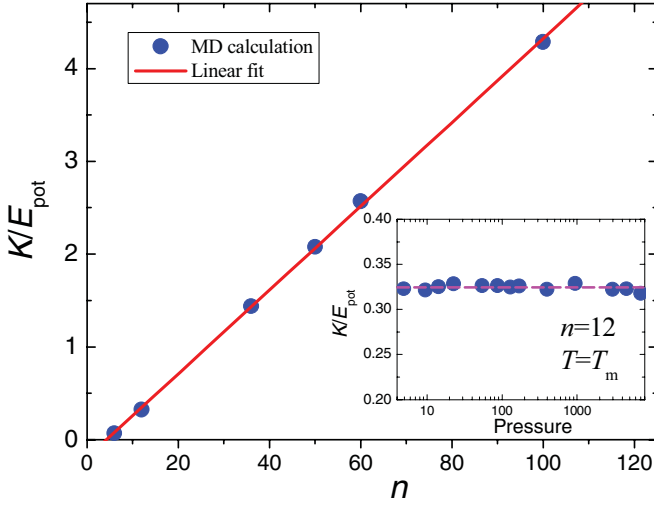


FIG. 9. (Color online) Kinetic-to-potential energy ratio for the SSp liquid at the melting curve (it is pressure independent) as a function of the soft-sphere potential exponent  $n$ . The inset shows the calculated pressure dependence of the kinetic-to-potential energy ratio at the melting curve for the SSp liquid with  $n = 12$  (the uncertainty of the calculation is on the order of the symbol size). Temperature and density are in standard soft-sphere units.

Formally, we note that particle motion for the hard-sphere system in the undercooled region can also be tentatively split into two types: a small amplitude motion inside the cages and rare jumps over large distances. Despite the similarity of this picture to the behavior of particle trajectories in a normal liquid, there are considerable distinctions. The hard-sphere motion inside the cages is of a purely collisional absolutely nonharmonic character, and the jumps only involve geometry restrictions rather than overcoming the activation barrier. In this case of  $c_V = 3/2k_B$ , the speed of sound and thermal speed

are not independent quantities, the structure corresponds to the random packing of spheres, and all transverselike excitations are damped at wavelengths on the order of one wavelength. Therefore, it is appropriate to treat the hard-sphere liquid as a nonrigid liquid at all temperatures.

The above results are important for understanding the difference between the liquid-glass transition and a jamming transition, the question that has been widely discussed and debated. For very large values,  $n > 100$ , the glass transition in an undercooled metastable melt occurs in a nonrigid liquid state and, like the hard-sphere glass transition, is governed by geometrical confinement conditions, and there is no temperature region with activated behavior.

It is known that the softer the repulsion potential, the lower the glass transition temperature or Kauzmann temperature [30,31]. Thus, the region of existence of the rigid liquid for the soft potential is wider both in the stable state over the melting temperature as well as in the metastable undercooled liquid state.

It is known that, for particle systems with a narrow region of the action of the potential, the liquid-gas equilibrium line in the equilibrium phase diagram is absent. Instead, there is a solid state crystal-crystal isostructural transition ending at the critical point [32–34]. In this case, the discussed Frenkel line, separating the harmonic and anharmonic states of the crystal, is, in fact, a continuation of the above isostructural transition into the supercritical region. Thus, for some colloidal and macromolecular systems for which the boiling line is absent, the Frenkel line can also lie in the region of stability of a solid phase.

## IX. THE FRENKEL LINE AGAINST THE WIDOM LINE

It is interesting to note the recent attempts [20,21] to link the change in the excitation spectrum to the “thermodynamic” continuation of the boiling curve, the so-called Widom line, the line of the maxima of thermodynamic properties in the vicinity of the critical point [35]. In Ref. [20], the Widom line was discussed for heat capacity only and, notably, experimental data were extrapolated at very high pressures to give an extrapolated thermodynamic line.

From the physical point of view, this extrapolated line is qualitatively different from the Frenkel line proposed here. Indeed, the proposed crossover line is not related to the extrapolation of the boiling curve and exists in systems where liquid-gas transition and the correspondent Widom line are absent altogether, including, in the model soft-sphere system, some colloidal systems, macromolecules, and so on [32–34]. In addition, there are several other important differences. First, the maxima of heat capacity  $c_P$  become smeared at  $T/T_c > 2.5$  and  $P/P_c > 15$  [12], and therefore, the extrapolation into the high pressure range ( $P/P_c \approx 100$ ) performed in Ref. [20] is not physically meaningful. Second, we have recently calculated compressibility  $\beta_T$ , expansion coefficient  $\alpha_P$ , heat capacity  $c_P$ , and density fluctuations  $\zeta$  along the isotherms for the Lennard-Jones particle system [36]. The results, together with experimental data for Ar and Ne, are summed up in Fig. 11. We observe that the thermodynamic continuation of the boiling curve gives a single line within 10% departure in temperature from the critical point only. Upon further departure, it represents a rapidly widening

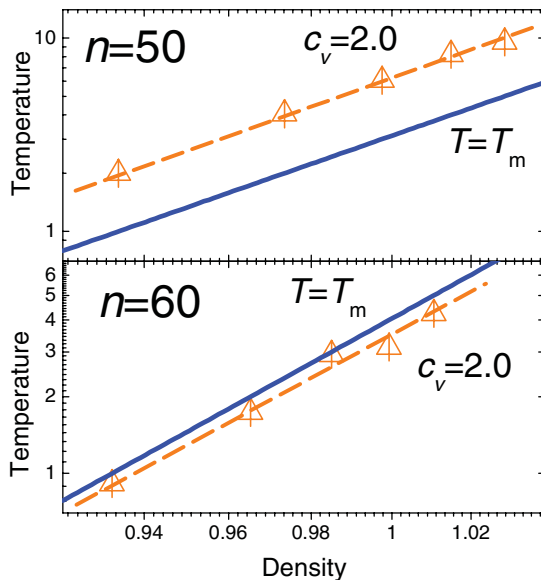


FIG. 10. (Color online) Relation between melting line (blue solid line) and line corresponding to the condition  $c_V = 2.0$  (orange symbols correspond to calculation, and orange dashed lines are approximations) for the SSp liquids with  $n = 50$  and  $60$ .



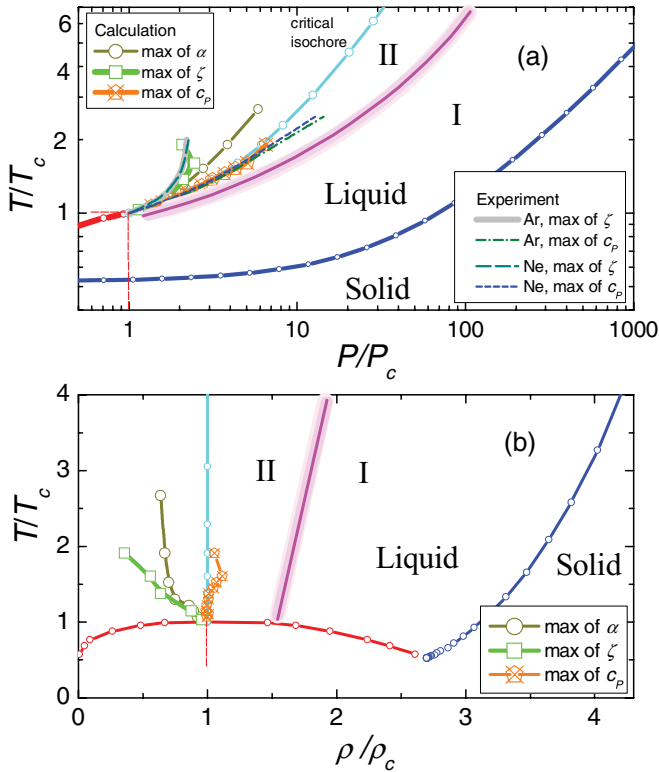


FIG. 11. (Color online)  $(T, P)$  and  $(T, \rho)$  phase diagrams of the simulated LJ liquid (the basic notations are the same as in Fig. 4 and the Frenkel line  $\tau \approx \tau_0$  and calculated detectable points of maximums for thermal expansion  $\alpha$ , fluctuations  $\zeta$ , and isobaric thermal capacity  $c_p$ . The similar experimental data for Ar and Ne [12] are shown in panel (a). The maximum of  $\beta$  becomes smeared at  $T > 1.1T_c$ , and its line is not shown.

bunch of lines instead of one single line, implying further that the extrapolation of the thermodynamic Widom line is not unique. Third, we observe that the lines of maximums of all calculated properties rapidly decrease in magnitude and become smeared at  $T > (2-2.5)T_c$  and  $P > (10-15)P_c$  and, therefore, cannot be meaningfully extrapolated to higher pressures and temperatures. This is in contrast to the proposed Frenkel line, which, as discussed above, exists for arbitrarily high pressures and temperatures. Finally, we note that, apart from the line of the maximums of the heat capacity lying close to the critical isochore, the lines of thermodynamic anomalies correspond to the decrease in density with a temperature increase, in strong contrast to the Frenkel line (Fig. 11).

## X. OTHER CROSSOVER LINES AND CONCLUSIONS

To summarize, we introduced the new line separating two liquid states with qualitatively different properties. We proposed to call the line, defined by Eq. (1), the Frenkel line to honor the contribution of Frenkel to the area of liquid dynamics. The contribution started from the microscopic definition and discussion of liquid relaxation time  $\tau$ . On the basis of this property, Frenkel made a number of important predictions regarding flow, relaxation, as well as elastic and phonon properties of liquids that subsequently formed the

microscopic basis of what is now known as the “viscoelastic” picture of liquids [1].

We note that the past few decades have seen considerable research into the undercooled metastable state of liquids related to the problem of glass transition. Several dynamic crossovers have been found that correspond to the mode-coupling temperature, the breakdown of the Stokes-Einstein relation, the crossover from exponential to nonexponential relaxation, between the Arrhenius and the Vogel-Fulcher-Tammann laws, and so on (see, e.g., Ref. [37] and references therein).

On the other hand, there have been no attempts to introduce a dynamic crossover at high temperatures that corresponds to a fundamental change in the character of atomic motion in a liquid. We note that the line partially related to our condition (2) was considered earlier, at least, at low pressures [38,39]. This line corresponds to percolation of “physical clusters.” A cluster, by definition, is made of particles linked pairwise where a pair of particles is linked if the sum of their relative kinetic and interaction energies is less than zero. This line may be not far from the Frenkel line only in the vicinity of the critical point. Rosenfeld also discussed a possible change in the nature of the dynamics of a simple liquid [40]. The corresponding crossover in Ref. [40] is reflected in a change from power law to exponential scaling of reduced transport coefficients when plotted versus excess entropy. In particular, Rosenfeld predicted a minimum of viscosity as a function of temperature for all inverse-power potentials. The crossover discussed in Ref. [40] has been obtained only at the low-density region where a weakly coupled liquid is considered to be close to a diluted gas with taking into account only first and second virial coefficients. Nevertheless, for SSp systems, at least at a small density region, the line of the crossover considered by Rosenfeld lies close to the Frenkel line. We also note the earlier paper of Hiwatari *et al.* [41], who found qualitatively different behaviors of the velocity autocorrelation function  $C(t)$  depending on the temperature and density for the SSp fluids [41]. For these systems, Hiwatari *et al.* assumed the existence of the critical reduced density that separated the liquidlike and gaslike dynamical regimes. For SSp with  $n = 12$ , Hiwatari *et al.* estimated the critical reduced density  $\rho^* \approx 0.54$  close to 0.58 found in our simulations for the same system. Unlike in the paper of Hiwatari *et al.*, the main parameter controlling the crossover in our theory was not density but relaxation time as given by our Eq. (1). In different systems, Eq. (1) gives different values of reduced density at the crossover.

As mentioned above, the concept of the Frenkel line may be applied to the colloidal liquids and macromolecular systems. In such complex systems, different time scales are present. There is some evidence of a mapping between long-time molecular and Brownian dynamics [42]. It is obvious that the dynamic rigid to non-rigid liquid transition should exist for the Brownian dynamics as well.

In conclusion, we state that the proposed Frenkel line separates a rigid liquid where solidlike shear waves exist and the diffusion regime is jumplike and is activated as in a solid from a nonrigid liquid where no shear modes exist and diffusion is collisional as in a gas. This line can be mapped in future experiments using several conditions for liquid properties that we discussed, including the disappearance of SROS peculiarities, the disappearance of the positive

dispersion of sound velocity, as well as specific values of diffusion constants, speed of sound, and specific heat:  $D \approx D_c$ ,  $V_s/V_{th} \approx 2$ , and  $c_V(T) \approx 2k_B$ .

### ACKNOWLEDGMENTS

The authors wish to thank S. M. Stishov, G. G. Simeoni, F. Gorelli, and H. E. Stanley for valuable discussions. This work has been supported by the RFBR (Grants No. 11-02-00303, No. 11-02-00341, and No. 10-02-01407) and by the Programs of the Presidium of RAS. K.T. is grateful to EPSRC.

### APPENDIX

We have studied the LJ liquid and two soft-sphere (SSp) liquids with  $n = 12$  and  $n = 6$  in a very wide range of parameters, from temperature  $T = 0.6$  (well below the critical point) to  $T = 100.0$  and densities from 0.1 to 2.7 for the LJ liquid,  $T = 0.1$ –100 and density in the range of 0.1–3.33 for the SSp liquid with  $n = 12$ , and  $T = 1.0$ –10 and density in the range of 0.5–4.5 for the SSp liquid with  $n = 6$ . We also have studied SSp liquids with high values of  $n$  up to 100 for the calculation of  $E_{pot}$  and  $c_V$ . An essential property of soft spheres is that the phase diagram corresponds to the equation  $\gamma = \rho \sigma^3 \left(\frac{\epsilon}{k_B T}\right)^{3/n} = \text{const}$ . The parameters  $\gamma$  for  $n = 12$  and  $n = 6$  systems were taken as  $\gamma_{12} = 1.15$  and  $\gamma_6 = 1.22$  [30]. System size in the simulations varied depending on the density reaching 4000 particles at the highest density. The cutoff radius was set at  $2.5\sigma$  for LJ and SSp with  $n = 12$  and half the box size for SSp with  $n = 6$ . The equations of state were integrated by the velocity Verlet algorithm. The temperature was kept constant during the equilibration by velocities rescaling. When the equilibrium was reached, the system was simulated in  $NVE$  ensemble. The usual equilibration period was  $1.5 \times 10^6$  steps, and the production run was  $0.5 \times 10^6$  steps where the time step was  $dt = 0.001$  LJ units. The soft-sphere system was simulated in  $NVE$  ensemble. The system consisted of 1000 particles, and the time step was 0.0005. The equilibration and production periods were  $3.5 \times 10^6$  and  $0.5 \times 10^6$  steps, respectively. The simulations and computation of properties were performed in the same way as for the LJ system. We also use the data of the potential energy and equation of state for the LJ fluid from Ref. [43] and the melting line of the LJ system from Ref. [44]. Everywhere in the text and in the figures, densities, temperatures, and pressures of the LJ liquid are given in the units  $\rho/\rho_c$ ,  $T/T_c$ , and  $P/P_c$ . The following critical parameters, averaged from literature sources, were used for the LJ system:  $\rho_c = 0.314$ ,  $T_c = 1.31$ .

To calculate the Debye period  $\tau_0$ , we analyzed many particle trajectories. At low temperatures,  $\tau_0$  was obtained as the average time of oscillatory motion at one equilibrium position of an atom before jumping to another position. At high temperatures, the oscillations disappear, and the motion of the particle consists of collisional movement only. The value of  $\tau$  was calculated as the time it takes a particle to move the distance close to the average interparticle separation. Then, it can be estimated as  $\tau = \frac{\rho^{-2/3}}{6D}$ , where  $D$  is the diffusion coefficient.  $D$  was calculated from the long-time limit of mean square displacement using the Einstein relation. We note that  $\tau_0$  can be obtained in the low-temperature limit where the oscillations are well pronounced, whereas,  $\tau$  can be calculated

from the diffusion value both at the low-temperature and at the high-temperature limit where there is a ballistic-collisional regime. It makes necessary to compute the values of  $\tau_0$  and  $\tau$  along the same isochores at different temperatures and extrapolate the data to see the cross points. The accuracy of the estimation of the temperature of crossover  $\tau = \tau_0$  is about  $\pm 20\%$ – $30\%$ ; the errors in the calculations of other values are less than 10%.

The values of  $\tau_0$  and  $\tau$  as well as the temperature of disappearance of solidlike vibration motion under heating also were extracted from the analysis of the self-intermediate scattering function  $F_s(q,t)$  and velocity autocorrelation function

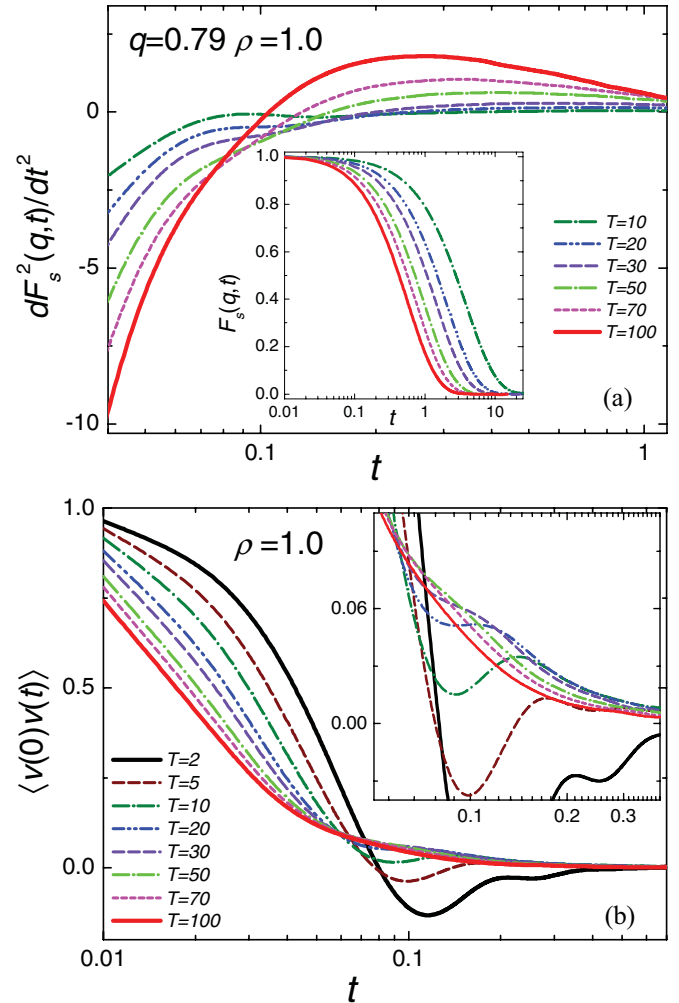


FIG. 12. (Color online) Self-intermediate scattering functions (in the inset) and (a) their second-order time derivatives and (b) velocity autocorrelation functions of the LJ liquid along the isochor  $\rho = 1$ . Temperature  $T$  is pointed out in LJ units. One can see the maxima of the second-order derivatives in panel (a). The maxima at shorter times correspond to the presence of vibrations, whereas, the maxima at larger times correspond to ballisticlike jumps. The disappearance of the maxima at the short time region occurs at  $T$  between 30 and 50, and it corresponds to the rigid liquid nonrigid liquid transition. Similarly, there are qualitative changes in the velocity autocorrelation function behavior in the same temperature region. Oscillations in the rigid liquid state take place, whereas, monotonic decay of autocorrelation functions in the nonrigid liquid state is observed.

$C(t)$  [15],

$$F_s(q, t) = \frac{1}{N} \left\langle \sum_{j=1}^N \exp[i\vec{q} \cdot (\vec{r}_j(t) - \vec{r}_j(0))] \right\rangle,$$

$$C(t) = \langle v(0)v(t) \rangle,$$

at different temperatures (see Fig. 12). Usually, the function  $F_s(q, t)$  is used to analyze the dynamics of glass-forming undercooled liquids [45,46]. However, more detailed analysis demonstrates that oscillating and ballistic-collisional regimes also can be seen from the behavior of these functions [47]. From Fig. 12, one can see qualitative changes in the self-intermediate scattering function and the velocity autocorrelation function at the same temperature interval around  $T \approx 30$  for  $\rho = 1$ .

The kinetic energy is obtained as  $K/N = 3k_B T/2$ , and the potential energy is obtained as the total energy of the interaction. In the case of the LJ liquid, there is a complication associated with the attractive part and the sign change in the potential energy at compression. That is why, in this case, we estimated the potential energy as  $E_{\text{pot}} = E_{\text{LJ}}(V) - E_{\text{LJ}}(V_0) + P_0(V_0 - V)$  where  $V_0$  corresponds to the volume of minimal possible (negative) pressure  $P_0$  at zero temperature.

Infinite-frequency shear modulus  $G_\infty$  was calculated as in Ref. [26] where it was shown that  $G_\infty$  for the pair-potential systems can be obtained from the radial distribution function. The bulk modulus  $B = \beta^{-1} = \rho \left( \frac{\partial \rho}{\partial P} \right)_T^{-1}$  was obtained from the equation of state. The longitudinal and transverse sound velocities were calculated as  $V_{\text{sl}} = (B/\rho)^{1/2}$  and  $V_{\text{st}} = (G_\infty/\rho)^{1/2}$ . The heat capacities at constant volume were obtained by differentiating the internal energy at isochors  $c_V = \left( \frac{\partial U}{\partial T} \right)_V$ .

The temperature corresponding to  $c_V = 2.0$  was determined from the dependence of the isochoric heat capacity on the temperature along the isochors by linear interpolation of the data. The same method was applied to construct other lines presented in our paper. Shear viscosity was computed by integrating the shear stress autocorrelation function.

The diffusion coefficients have been calculated from the viscosity data using the Stokes-Einstein relationship. To prove condition (3) for real liquids, we have taken the relationship  $V_{\text{sl}} = 2.3 V_{\text{th}}$  [where the coefficient 2.3 for the longitudinal sound velocity instead of 2 for the shear sound velocity was taken to match with condition (5) for the same systems at  $P \sim 100 P_c$ ]. Thermodynamic and dynamic data for real fluids (Ar, Ne, and  $\text{N}_2$ ) were taken from Ref. [12].

- 
- [1] J. Frenkel, *Kinetic Theory of Liquids* (Oxford University Press, New York, 1946).
- [2] J. C. Maxwell, *Philos. Trans. R. Soc. London* **157**, 49 (1867).
- [3] D. C. Wallace, *Phys. Rev. E* **56**, 4179 (1997).
- [4] E. D. Chisolm and D. C. Wallace, *J. Phys.: Condens. Matter* **13**, R739 (2001).
- [5] M. Grimsditch, R. Bhadra, and L. M. Torell, *Phys. Rev. Lett.* **62**, 2616 (1989).
- [6] T. Pezeril, C. Klieber, S. Andrieu, and K. A. Nelson, *Phys. Rev. Lett.* **102**, 107402 (2009).
- [7] S. Hosokawa *et al.*, *Phys. Rev. Lett.* **102**, 105502 (2009).
- [8] Y. Jeong, S. R. Nagel, and S. Bhattacharya, *Phys. Rev. A* **34**, 602 (1986).
- [9] C. J. Roberts, A. Z. Panagiotopoulos, and P. G. Debenedetti, *Phys. Rev. Lett.* **77**, 4386 (1996).
- [10] *New Kinds of Phase Transitions: Transformations in Disordered Substances, Proceedings of NATO Advanced Research Workshop, Volga River*, edited by V. V. Brazhkin, S. V. Buldyrev, V. N. Ryzhov, and H. E. Stanley (Kluwer, Dordrecht, 2002).
- [11] P. F. McMillan, *J. Mater. Chem.* **14**, 1506 (2004).
- [12] *NIST Chemistry WebBook* [<http://webbook.nist.gov/chemistry/>].
- [13] S. M. Stishov, *JETP Lett.* **57**, 196 (1993).
- [14] J. P. Boon and S. Yip, *Molecular Hydrodynamics* (McGraw-Hill International Book Company, New York, 1980).
- [15] U. Balucani and M. Zoppi, *Dynamics of the Liquid State* (Clarendon, Oxford, 1994).
- [16] E. Pontecorvo, M. Krisch, A. Cunsolo, G. Monaco, A. Mermet, R. Verbeni, F. Sette, and G. Ruocco, *Phys. Rev. E* **71**, 011501 (2005).
- [17] T. Bryk *et al.*, *J. Chem. Phys.* **133**, 024502 (2010).
- [18] W-C. Pilgrim and C. Morcel, *J. Phys.: Condens. Matter* **18**, R585 (2006).
- [19] T. Scopigno, G. Ruocco, and F. Sette, *Rev. Mod. Phys.* **77**, 881 (2005).
- [20] G. G. Simeoni *et al.*, *Nat. Phys.* **6**, 503 (2010).
- [21] F. Gorelli, M. Santoro, T. Scopigno, M. Krisch, and G. Ruocco, *Phys. Rev. Lett.* **97**, 245702 (2006).
- [22] F. Bencivenga *et al.*, *Europhys. Lett.* **75**, 70 (2006).
- [23] F. Bencivenga, A. Cunsolo, M. Krisch, G. Monaco, L. Orsingher, G. Ruocco, F. Sette, and A. Vispa, *Phys. Rev. Lett.* **98**, 085501 (2007).
- [24] F. Bencivenga *et al.*, *J. Chem. Phys.* **130**, 064501 (2009).
- [25] C. R. Reid and T. K. Sherwood, in *The Properties of Gases and Liquids*, 2nd ed. (McGraw-Hill, New York, 1966).
- [26] R. Zwanzig and R. D. Mountain, *J. Chem. Phys.* **43**, 4464 (1965).
- [27] G. Grimvall, *Phys. Scr.* **11**, 81 (1975).
- [28] K. Trachenko, *Phys. Rev. B* **78**, 104201 (2008).
- [29] W. G. Hoover, S. G. Gray, and K. W. Johnson, *J. Chem. Phys.* **55**, 1128 (1971).
- [30] D. M. Heyes and A. C. Branka, *Mol. Phys.* **107**, 309 (2009).
- [31] Z. Shi, P. G. Debenedetti, F. H. Stillinger, and P. Ginart, *J. Chem. Phys.* **135**, 084513 (2011).
- [32] G. Malescio, *J. Phys.: Condens. Matter* **19**, 073101 (2007).
- [33] M. H. J. Hagen *et al.*, *Nature (London)* **365**, 425 (1993).
- [34] A. P. Gast and W. B. Russel, *Phys. Today* **51**(12), 24 (1998).
- [35] L. Xu *et al.*, *Proc. Natl. Acad. Sci. USA* **102**, 16558 (2005).
- [36] V. V. Brazhkin *et al.*, *J. Phys. Chem. B* **115**, 14112 (2011).
- [37] F. Mallamace *et al.*, *Proc. Natl. Acad. Sci. USA* **107**, 22457 (2010).
- [38] A. Coniglio, U. De Angelis, and A. Forlani, *J. Phys. A* **10**, 1123 (1977).
- [39] X. Campi, H. Krivine, and N. Sator, *Physica A* **296**, 24 (2001).

- [40] Y. Rosenfeld, *J. Phys.: Condens. Matter* **11**, 5415 (1999).
- [41] Y. Hiwatari *et al.*, *Progr. Theor. Phys.* **52**, 1105 (1974).
- [42] M. J. Pond, J. R. Errigton, and T. M. Truskett, *Soft Matter* **7**, 9859 (2011).
- [43] K. Meier, Ph.D. thesis, University of the Federal Armed Forces Hamburg, 2002.
- [44] R. Agrawal and D. A. Kofke, *Mol. Phys.* **85**, 43 (1995).
- [45] W. Kob and H. C. Andersen, *Phys. Rev. Lett.* **73**, 1376 (1994).
- [46] T. B. Schroder, S. Sastry, J. C. Dyre, and S. C. Glotzer, *J. Chem. Phys.* **112**, 9834 (2000).
- [47] G. De Lorenzi-Venneri, E. D. Chisolm, and D. C. Wallace, *Phys. Rev. E* **78**, 041205 (2008).